Heat treatment of bearing steels: an industrial investigation

A. Fortini, L. Bocchi, M. Merlin, E. Bertarelli

Bearings are critical components used in rotating machinery to enable motion with minimal friction for which the material and, in turn, the heat treatment selection are crucial. The heat treatment typically involves austenitization followed by cooling to achieve the desired microstructure and hardness. In this study, the effects of process parameters during different salt quenching heat treatment routes on two bearing steels (EN 100Cr6 and EN 100CrMo7) were investigated, focusing on the industrial austempering of high-thickness rings, to achieve a bainitic structure with high toughness. Hardness evolution and microstructural changes were analyzed to test the efficacy of the isothermal heat treatment for different steels and on varying the geometry of the components. The results provide a basis for selecting an effective industrial austempering process for different steel and part geometries.

KEYWORDS: BEARING STEELS, AUSTEMPERING, MICROSTRUCTURE, HARDNESS, BAINITE

INTRODUCTION

Bearings consist of rolling elements (balls, cylinders, or barrel shapes) and rings that enable one part to rotate or move in contact with another with as little friction as possible. The proper material for this application has been widely investigated, and there has been over a century of work on alloys for rolling bearings [1–3]. Despite that, the topic is still of great interest and with many unresolved issues [2,4–6].

Of the many alloys that have been studied in the history of bearing steels, there are only two categories of steels that find application in the majority of bearings: those which are hardened throughout their sections into the martensitic or bainitic condition and others that have soft and tough cores, but hard surface layers induced using processes such as a case hardening or induction hardening [7].

The typical through-hardening heat treatment for bearing steels consists of heating above the austenitization temperature until the structure is fully austenitic and most of the carbides are dissolved in the matrix, then cooling the material with the proper cooling speed to achieve the desired microstructure and hardness [8]. If a martensitic microstructure is desired, cooling speed should be high in order to avoid every other phase transformation at higher temperatures and be able to cross both Ms (Martensite start) and Mf (Martensite finish) temperatures. When a martensitic structure is obtained, usually a subsequent tempering is required to recover toughness at the expense

A. Fortini, L. Bocchi, M. Merlin
Department of Engineering (DE) – University of Ferrara

E. Bertarelli
Timaf Snc

of hardness. Martensitic quenching from austenitization temperature usually leads to a microstructure containing martensite, about 6 vol. % of retained austenite and 3 - 4 vol. % of cementite particles that have failed to dissolve during austenitization. Martensitic quenching is not necessarily the chosen treatment for bearing steels. The heat transfer during quenching routes drives the microstructural evolution and development of stress and strain in the material. Non-uniform heat transfer at the surface creates a thermal gradient on the surface and within the quenched component. The phase transformations lead to distortions, i.e. dimensional variation or changes, that require further machining operations with additional time and costs. Hence, to obtain increased toughness, reduced expansion during transformation and minimization of quench cracking occurrence, austempering is preferred [9]. The austempering process is known to reduce distortions through the formation of a bainitic structure, however, its application to large-scale components in industrial practice is rarely studied. Residual stresses and distortions, as well as the kinetic of the quench phase transformations, are widely investigated; nevertheless, the connection among them has not been deeply analyzed [10].

Against this background, the present study seeks to examine the effects of process parameters during industrial isothermal heat treatment routes applied on two bearing steels (EN 100Cr6 and EN 100CrMo7) in terms of microstructural and hardness changes.

MATERIALS AND METHODS

This study is focused on components made of two traditional bearings steels (EN 100Cr6 and EN 100CrMo7) manufactured from steel pipes from Ovako AB, Sweden. Figure 1 shows the investigated components: as for the EN 100Cr6, the rings are 18 mm thick and 36 mm in height with an outer diameter of 164 mm, while the EN 100CrMo7 ones are 32 mm thick and 64 mm in height with an outer diameter of 132 mm. The simplified geometry of parts (with no tracks and other detail features) is fully representative of real components with high wall thickness that is at the upper limit (for EN 100Cr6 parts) or even exceeding the upper limit (for EN 100CrMo7 parts), considering hardenability reported, for example, on supplier technical information sheets [11]. The chemical composition of the steels, analyzed by the G.N.R. S7 Metal Lab Plus (G.N.R., Agrate Conturbia, Italy) quantimeter, is reported in Table 1 and Table 2.

Fig.1 - Image of the investigated bearing rings.

Tab.1 - Chemical composition (wt.%) of the investigated EN 100Cr6 steel.

Chemical composition (wt.%) – Fe balance										
	C	Si	Mn	P	S	Cr	Mo	Ni	Al	Cu
Mean	0.999	0.306	0.341	0.006	0.008	1.396	0.044	0.177	0.007	0.213
St. Dev.	0.009	0.003	0.005	0.001	0.002	0.050	0.002	0.004	0.002	0.006

Tab.2 - Chemical composition (wt.%) of the investigated EN 100CrMo7 steel

Chemical composition (wt.%) – Fe balance										
	C	Si	Mn	P	S	Cr	Mo	Ni	Al	Cu
Mean	0.959	0.300	0.295	0.011	0.010	1.649	0.181	0.192	0.024	0.178
St. Dev.	0.018	0.017	0.010	0.002	0.003	0.023	0.008	0.006	0.006	0.008

At first, microstructural investigation and Brinell hardness tests on the as-received materials were done. The analyses comprised the standard metallographic procedures, while the final chemical etching was performed through Nital 4 % (4 % HNO_3 in ethanol) reagent. Micrographs were carried out by a Zeiss EVO MA15 (Carl Zeiss, Jena, Germany) scanning electron microscope. Images were recorded in backscattered electron imaging (BSE-SEM) mode. The mean Brinell hardness was determined under a 187.5 kgf load and with a 2.5 mm diameter spherical indenter (HBW 2.5/187.5) with the AT130D Ernst (Cisam-Ernst, Induno Olona, Italy) hardness tester, in agreement with the UNI EN ISO 6506 standard. The mean value was calculated as an average of five randomly acquired indentations along the ring's thickness.

Then, the effects of isothermal heat treatment routes on the microstructural characteristics and hardness were investigated. In this study, the austenitization temperature is selected to be 5 °C above the maximum value suggested by supplier datasheets [12,13]. The first route was performed as follows: three rings of EN 100Cr6 and three rings of EN 100CrMo7 were pre-heated and austenitized at 880 °C for 150 min in an Albaplant FP 120.200 C-A (Albaplant Srl, Pessano con Bornago, Italy) pit furnace. The rings were thus transferred into a salt bath settled at 240 °C, and three holding times in the molten bath were considered, i.e. 60 min, 150 min and 300 min. Finally, all the rings were air-cooled to room temperature and subsequently tempered at 230 °C for 120 min. The second route comprised the same austenitization procedure while the salt bath was held at 220 °C. Figure 2 represents the investigated isothermal heat treatment routes on both EN 100Cr6 and EN 100CrMo7 rings.

Microstructural analyses were conducted on a longitudinal section of each ring, i.e. along the ring's height, and in the center of the ring's thickness. The investigated sections were: the upper surface of the ring (i.e. the last that faced the quenching medium), the lower surface (i.e. the first that faced the quenching medium) and the central region (i.e. half the height of the ring). The analyses comprised the above-described standard metallographic procedures and SEM investigation. Images were recorded in secondary electron imaging (SE-SEM) mode. On the heat-treated samples, the Rockwell C hardness (HRC) was evaluated by the AT130D Ernst hardness tester in agreement with the UNI EN ISO 6508 standard. HRC tests were carried out on the longitudinal section, considering hardness evolution from the upper to the lower surface and in the center of the ring's thickness.

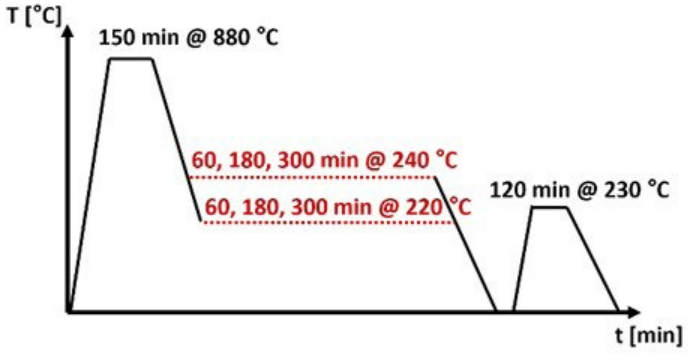

Fig.2 - Scheme of the two investigated heat treatment routes.

La Metallurgia Italiana
International Journal of the Italian Association for Metallurgy

RESULTS AND DISCUSSION

Microstructural investigations on the as-received materials revealed a microstructure composed of globular cementite uniformly distributed throughout the ferritic matrix, consistent with a spheroidizing annealing heat treatment. Such treatment promotes the workability of the material. There were no remarkable differences between the investigated regions along the longitudinal section and between the two analyzed steels, confirming the homogeneity of the microstructure. Figure 3 displays the SE-SEM micrographs of the EN 100Cr6 (Fig. 3a) and the EN 100CrMo7 (Fig. 3b) steel from which the spherical carbides can be detected. The as-received rings had a mean hardness of 207 ± 2 HBW and 209 ± 1 HBW for the EN 100Cr6 and EN 100Cr6 ring, respectively. Such values are in accordance with the hardness usually required for bearing steels after spheroidizing annealing treatment [1].

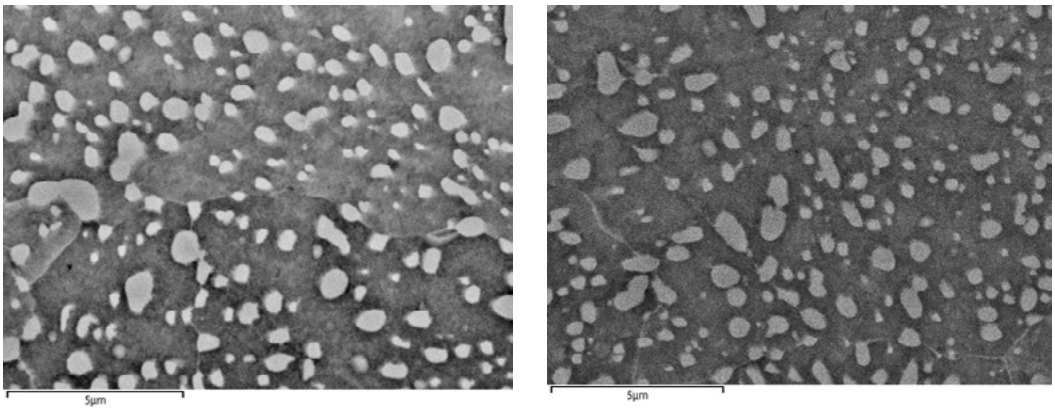

(a) (b)

Fig.3 - SE-SEM micrographs of the as-received materials: (a) EN 100Cr6 steel; (b) EN 100CrMo7 steel.

Figures 4 and 5 summarize the measured HRC evolution along the ring's height for the EN100Cr6 and the EN 100CrMo7 steel, respectively. Focusing on the EN 100Cr6 steel, it can be observed that the temperature of the salt bath does not significantly affect the hardness evolution. Regardless of the dwelling time, HRC values are in the range of 59.5 HRC and 62.0 HRC for the 240 °C isothermal treatment and in the range of 60.0 HRC and 63.0 HRC for the 220 °C isothermal treatment. From the comparison between the two isothermal treatments, it can be observed slightly higher hardness values for the lower investigated temperature, as also confirmed in the literature [8,14]. Concerning the investigated dwelling times, no specific trend was detected from 60 min up to 300 min. On the contrary, for all the investigated conditions, the HRC evolution from the upper/lower surface of the ring to the central region shows a reduction of up to 2.0 HRC points. Regarding the EN 100CrMo7 steel, some differences in comparison with the EN 100Cr6 steel are evident. As alre-ady observed, regardless of the investigated dwelling times, the higher the temperature of the salt bath, the lower the HRC values [8]. In addition, the 240 °C isothermal treatment shows a variation in the HRC values from the upper/lower surface of the ring to the central region of up to 4.0 HRC points. As previously outlined for EN 100Cr6 steel, the influence of dwelling time on HRC values does not follow any specific trend, also because, for the EN 100CrMo7 steel, data are, on average, less scattered.

These results can be commented on by correlating experimental findings with different material hardenability and ring geometries. In general, it is not surprising that the upper/lower surfaces always show higher hardness values than the center. Considering the low thermal conductivity of these alloyed steels and, consequently, the high-slope thermal gradients with a linear decrement of temperature with distance [15], different cooling laws arise for the different material locations. More specifically, EN 100Cr6 ring has a thickness of 18 mm, just above the hardenability limit of 17 mm indicated by the supplier [11], explaining the small gap in hardness from surface to core. In turn, although EN 100Cr7 has a higher

quench penetration depth [13], the thickness of the ring of 32 mm largely exceeds the safe hardenability limit of 20 mm suggested by the supplier [11]. This intentional choice in our study is to represent a typical case in bearing components heat treatment in production, where materials are sometimes used above the nominal range of application in terms of hardenability.

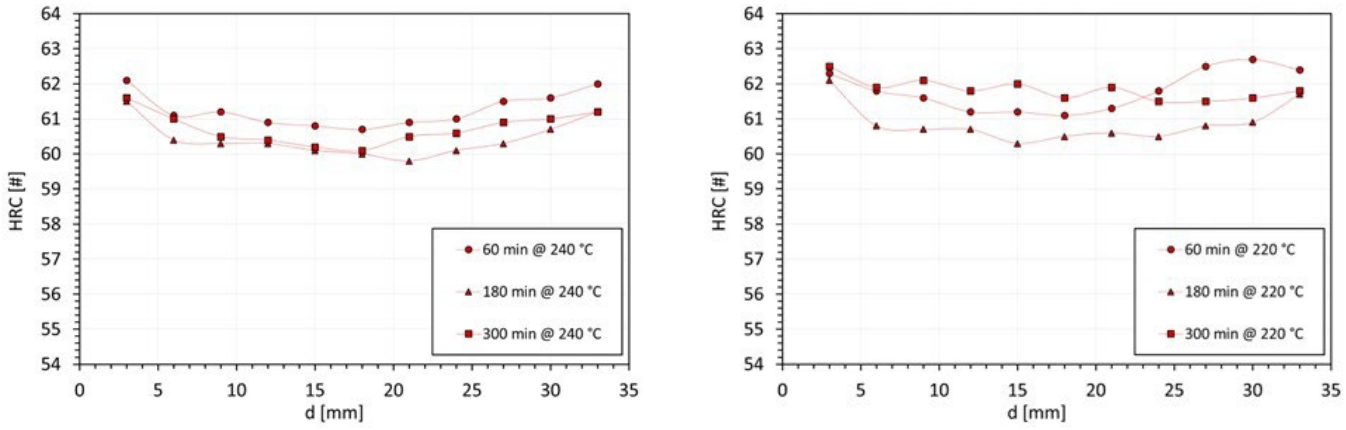

(a) (b)

Fig.4 - HRC evolution against the "d" ring's height for the EN 100Cr6 steel: (a) austenitization at 880 °C + isothermal treatment at 240 °C for 60 min, 180 min and 300 min + tempering at 230 °C for 120 min; (b) austenitization at 880 °C + isothermal treatment at 220 °C for 60 min, 180 min and 300 min + tempering at 230 °C for 120 min.

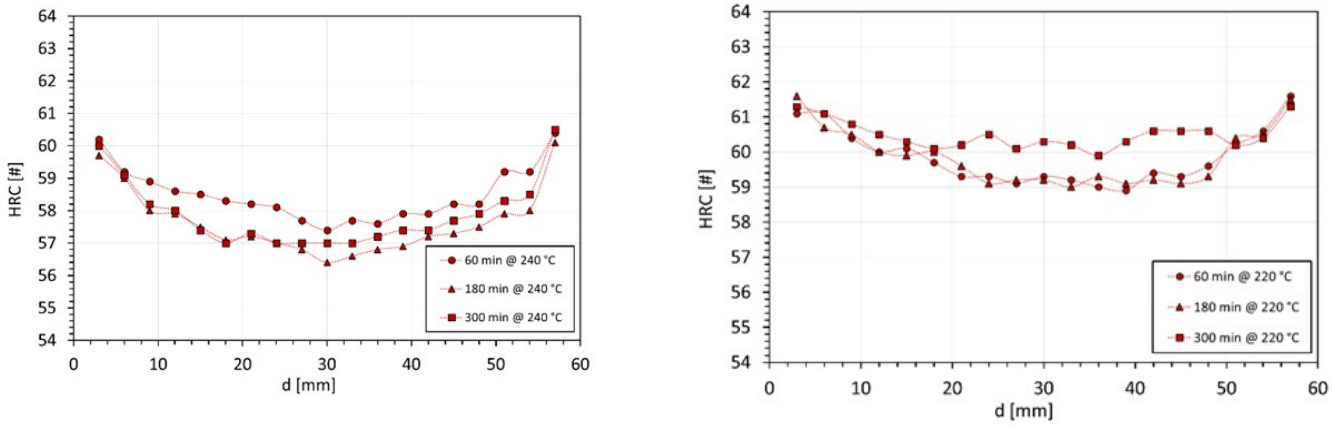

(a) (b)

Fig.5 - HRC evolution against the "d" ring's height for the EN 100CrMo7 steel: (a) austenitization at 880 °C + isothermal treatment at 240 °C for 60 min, 180 min and 300 min + tempering at 230 °C for 120 min; (b) austenitization at 880 °C + isothermal treatment at 220 °C for 60 min, 180 min and 300 min + tempering at 230 °C for 120 min.

Figures 6 and 7 report the SEM micrographs of the EN 100Cr6 steel austenitized at 880 °C for 150 min and cooled in the salt bath at 220 °C and at 240 °C, respectively. As seen, the heat treatment route promoted the carbide dissolution that is dependent on the austenitization temperature and time and affects the bainitic transformation [6]. Regardless of the dwelling temperature and time, the observed microstructures were almost entirely bainitic. Based on the above-described experimental findings, the comparison between the 60 min and 300 min dwelling times is reported. For both the 220 °C (Fig. 6) and the 240 °C (Fig. 7) salt bath temperatures, the 60 min (Fig. 6a and 6c; Fig. 7a and 7c) and 300 min dwelling times (Fig. 6b and 6d; Fig. 7b and 7d) show a homogeneous bainite microstructure where the acicular structure of upper bainite with fine carbide precipitation within the ferrite plate is detectable. Such evidence, coupled with the HRC data (Fig. 4) suggests that bainite transformation was completed after 60 min. From

the comparison between the upper surface of the ring (Fig. 6a and b; Fig. 7a and 7b) and the central region (Fig. 6c and 6d; Fig. 7c and 7d), any noticeable changes in the SE-SEM micrographs were detected. Hence, the coupled HRC values and the SEM investigations suggest that the proposed heat treatment routes provided comparable behaviors for the considered part geometry.

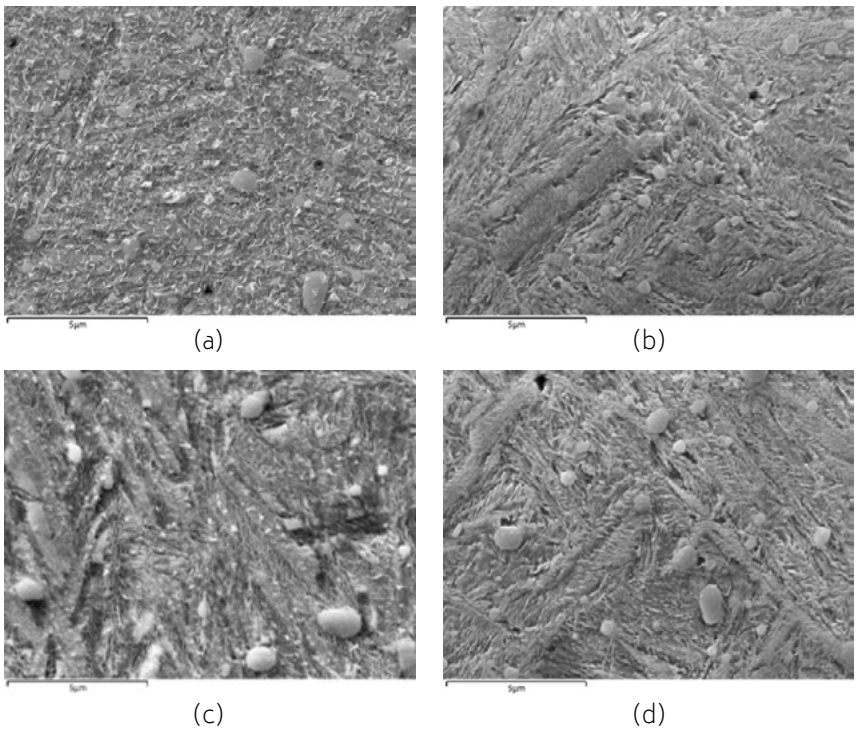

Fig.6 - SE-SEM micrographs of the EN 100Cr6 steel austenitized at 880 °C for 150 min + salt quenching at 240 °C: (a) 60 min holding time in the upper surface of the ring, (b) 300 min holding time in the upper surface of the ring, (c) 60 min holding time in the central region of the ring, (d) 300 min holding time in the central region of the ring

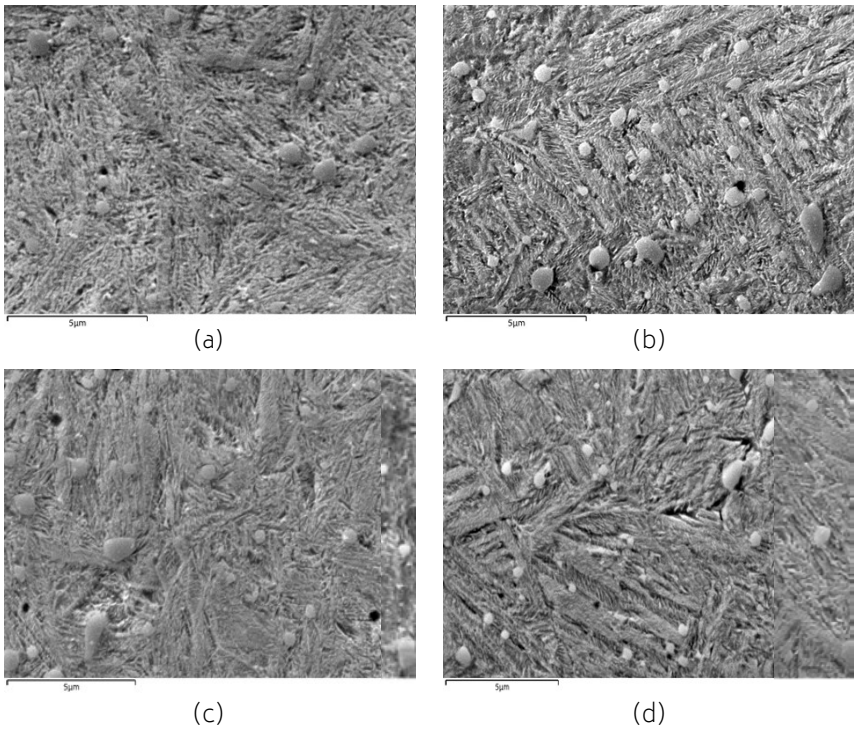

Fig.7 - SE-SEM micrographs of the EN 100Cr6 steel austenitized at 880 °C for 150 min + salt quenching at 220 °C: (a) 60 min holding time in the upper surface of the ring, (b) 300 min holding time in the upper surface of the ring, (c) 60 min holding time in the central region of the ring, (d) 300 min holding time in the central region of the ring

Concerning the EN 100CrMo7 steel, the SEM micrographs of the rings austenitized at 880 °C for 150 min and cooled in the salt bath at 240 °C and at 220 °C are summarized in Fig. 8 and Fig. 9, respectively. The spheroidized carbides amount is overall higher with respect to EN 100Cr6 steel and affects the phase transformation [5]. Similarly to the EN 100Cr6 steel, the EN 100CrMo7 steel is almost entirely bainitic for all the investigated heat treatment routes. Conversely, remarkable differences between the upper surface of the ring (Fig. 8a and 8b; Fig. 9a and 7b) and the central region (Fig. 8c and 8d; Fig. 9c and 9d) can be observed. In the central region of the rings held at 240 °C for 60 min (Fig. 8c) and for 300 min (Fig. 8d), the SE-SEM micrographs revealed the presence of large regions similar to upper bainite structures, where larger cementite carbides are detectable, suggesting a mixture of upper and lower bainite microstructure. Such evidence matches the above-reported HRC evolution along the ring's height. Similarly, from the SEM microstructures of the rings austenitized at 880 °C for 150 min and cooled in the salt bath at 220 °C (Fig. 9), the upper surface of the ring shows a homogeneous microstructure composed of lower bainite. It is worth noting that this microstructure appears coarser than the one observed for the salt bath at 240 °C (Fig. 8) but with an appreciable coarsening effect of spheroidal carbides, which can explain the slightly higher HRC values in the upper/lower regions of the rings (Fig. 5b). Regarding the central regions (Fig. 9c and 9d) some amount of upper bainite can be detected but less than the ones observed for the salt bath at 240 °C (Fig. 8c and 8d). As a result, the heat treatment route comprising the salt bath quenching at 220 °C appeared most efficient for the investigated EN 100CrMo7 ring.

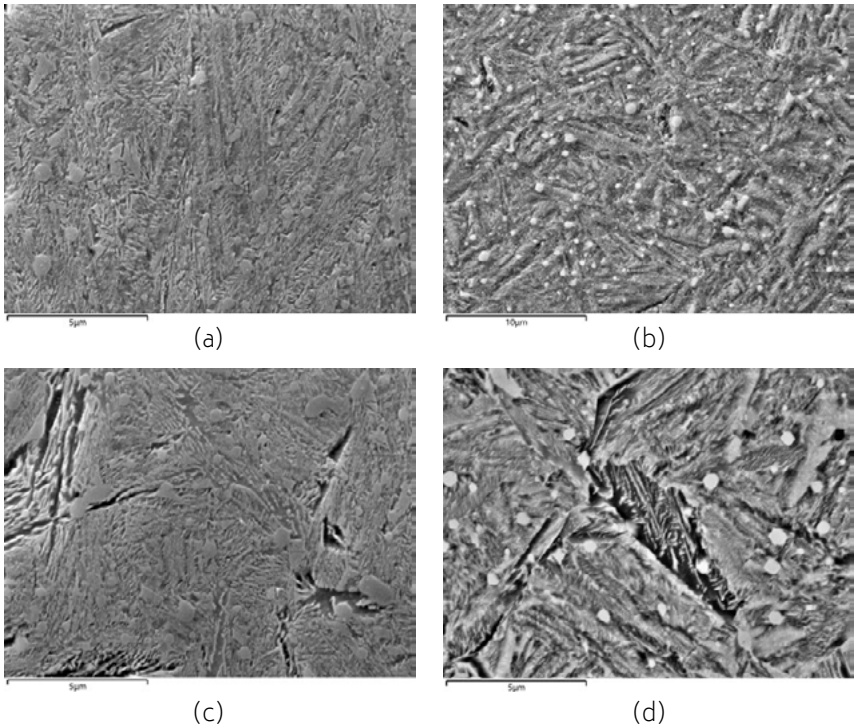

Fig.8 - SE-SEM micrographs of the EN 100CrMo7 steel austenitized at 880 °C for 150 min + salt quenching at 240 °C: (a) 60 min holding time in the upper surface of the ring, (b) 300 min holding time in the upper surface of the ring, (c) 60 min holding time in the central region of the ring, (d) 300 min holding time in the central region of the ring

La Metallurgia Italiana
International Journal of the Italian Association for Metallurgy

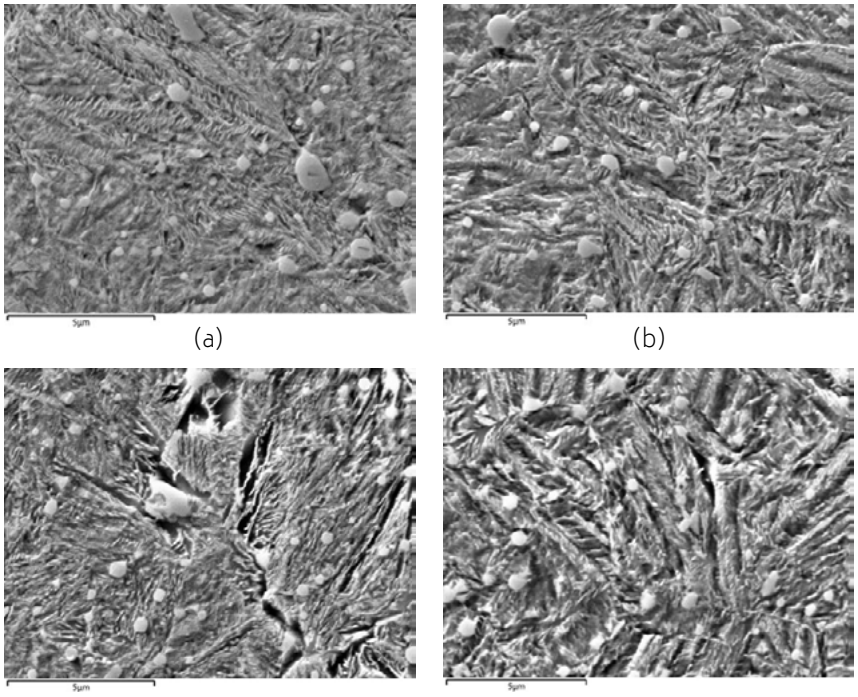

Fig.9 - SE-SEM micrographs of the EN 100CrMo7 steel austenitized at 880 °C for 150 min + salt quenching at 220 °C: (a) 60 min holding time in the upper surface of the ring, (b) 300 min holding time in the upper surface of the ring, (c) 60 min holding time in the central region of the ring, (d) 300 min holding time in the central region of the ring

CONCLUSIONS AND OUTLOOKS

This study provided insights into the resulting microstructure and hardness of two widely used through hardening bearing steels after executing austempering trials on parts with geometries that are truly representative of real industrial cases.

EN 100Cr6 ring is characterized by a geometry that is at the limit of material hardenability declared by the supplier. The resulting microstructure is fully bainitic for all considered process routes, while hardness variation from surface to core is below 2.0 HRC points, compatible with standard through hardening design specifications.

EN 100CrMo7 ring wall thickness is significantly above the material hardenability limit (+ 60 % thickness compared to the safe hardenability limit for this material). This condition represents an attempt to use the material above the nominal range of application in terms of hardenability by improving knowledge and control of heat treatment parameters. This allows the heat treatment factory to support the customers to minimize final costs by avoiding more expensive materials with higher hardenability. This requires a rigorous approach, supported by mechanical characterization and micrographic investigations to determine the actual achieved result.

For the 32 mm thick EN 100CrMo7 rings, a heat treatment route implying austenitization at 880 °C for 150 min followed by isothermal treatment at 220 °C and final tempering at 230 °C provided a bainitic microstructure with hardness variation from surface to core not exceeding 4.0 HRC points. This is an interesting result from an industrial perspective, but further studies are ongoing by evaluating different austenitization parameters and different austempering parameters. The dimensional variations of parts subjected to through hardening is an additional topic to be addressed by combining the industrial perspective with applied research. To this aim, we believe that a deeper investigation of microstructure and phase transformations during the entire heat treatment route can provide more insights.

REFERENCES

[1] T.A. Harris, W.J. Anderson, Rolling Bearing Analysis, J. Lubr. Technol. 89 (1967) 521–521. https://doi.org/10.1115/1.3617048.
[2] H.K.D.H. Bhadeshia, Steels for bearings, Prog. Mater. Sci. 57 (2012) 268–435. https://doi.org/10.1016/j.pmatsci.2011.06.002.
[3] F.J. Ebert, Fundamentals of Design and Technology of Rolling Element Bearings, Chinese J. Aeronaut. (2010). https://doi.org/10.1016/S1000-9361(09)60196-5.
[4] D. Foster, M. Paladugu, J. Hughes, M. Kapousidou, U. Islam, A. Stark, N. Schell, E. Jimenez-Melero, Formation of lower bainite in a high carbon steel - An in-situ synchrotron XRD study, J. Mater. Res. Technol. (2022). https://doi.org/10.1016/j.jmrt.2022.05.025.
[5] M. El Laithy, L. Wang, T.J. Harvey, B. Vierneusel, M. Correns, T. Blass, Further understanding of rolling contact fatigue in rolling element bearings - A review, Tribol. Int. (2019). https://doi.org/10.1016/j.triboint.2019.105849.
[6] H. Li, M. Xu, Z.T. Li, Transformation behavior and acceleration of low-temperature bainite in high carbon chrominum steel, Mater. Res. Express. (2018). https://doi.org/10.1088/2053-1591/aad167.
[7] J.L. Dossett, Practical Heat Treating, 2020. https://doi.org/10.31399/asm.tb.phtbp.9781627083263.
[8] Y. Pan, B. Wang, G.C. Barber, Study of bainitic transformation kinetics in SAE 52100 steel, J. Mater. Res. Technol. 8 (2019) 4569–4576. https://doi.org/10.1016/j.jmrt.2019.08.001.
[9] P.V. Krishna, R.R. Srikant, M. Iqbal, N. Sriram, Effect of Austempering and Martempering on the Properties of AISI 52100 Steel, ISRN Tribol. (2013). https://doi.org/10.5402/2013/515484.
[10] J. Chakraborty, D. Bhattacharjee, I. Manna, Austempering of bearing steel for improved mechanical properties, Scr. Mater. (2008). https://doi.org/10.1016/j.scriptamat.2008.03.023.
[11] Ovako, Standard Bearing tube - technical data, (n.d.).
[12] Ovako, Material data sheet - Steel grade 100Cr6, (n.d.).
[13] Ovako, Material data sheet - Steel grade 100CrMo7, (n.d.).
[14] Y. Wang, T.C. Lei, C.Q. Gao, Influence of isothermal hardening on the sliding wear behaviour of 52100 bearing steel, Tribol. Int. 23 (1990) 47–53. https://doi.org/10.1016/0301-679X(90)90072-W.
[15] G.B. Arfken, D.F. Griffing, D.C. Kelly, J. Priest, Heat transfer, in: Int. Ed. Univ. Phys., Elsevier, 1984: pp. 430–443. u https://doi.org/10.1016/B978-0-12-059858-8.50028-5.

TORNA ALL'INDICE >